

Electrocaloric Effect in Ferroelectric Rochelle Salt

GORDON G. WISEMAN AND JUERGEN K. KUEBLER

The University of Kansas, Lawrence, Kansas

(Received 1 April 1963; revised manuscript received 20 May 1963)

Measurements of the electrocaloric effect in crystalline Rochelle salt throughout the ferroelectric range have been made and have been used to determine the Devonshire "dielectric stiffness" coefficient, the ferroelectric Curie temperatures, and the spontaneous polarization close to both Curie temperatures. The results are shown to be consistent with the thermodynamic properties of Rochelle salt as determined from measurements of the spontaneous polarization and the low-field differential susceptibility.

INTRODUCTION

GENERAL thermodynamic considerations give alternative expressions for the reversible electrocaloric effect¹:

$$dT = -(T/C_E)(\partial P/\partial T)_E dE, \quad (1a)$$

$$dT = (T/C_P)(\partial E/\partial T)_P dP. \quad (1b)$$

Here P is the electric polarization per unit volume, T is the absolute temperature, and E is the applied electric field; C_P and C_E are the heat capacities per unit volume at constant polarization and constant field. To evaluate the partial differential coefficients in (1a) and (1b), the elastic Gibbs function^{2,3} is expanded in powers of P ,

$$G = G_0(T) + \frac{1}{2}\chi_0(T)P^2 + \frac{1}{4}\xi P^4 + \frac{1}{6}\zeta P^6 + \dots \quad (2)$$

and

$$dG = -SdT + EdP, \quad (3)$$

where G_0 is the free energy of the unpolarized crystal, χ_0 is called by Devonshire the "dielectric stiffness" coefficient, and the coefficients (ξ, ζ, \dots) of the higher order terms are taken to be positive for a substance which undergoes a second-order phase transition. In first approximation, the latter coefficients are independent of temperature. From Eqs. (3) and (2),

$$E = (\partial G/\partial P)_T = \chi_0 P + \xi P^3 + \zeta P^5 + \dots, \quad (4)$$

and

$$(\partial E/\partial T)_P = (\partial \chi_0/\partial T)_P P,$$

and Eq. (1b) becomes

$$dT = (T/C_P)(\partial \chi_0/\partial T)_P P dP. \quad (5)$$

Therefore, quantitative electrocaloric measurements will give the variation of χ_0 with temperature, particularly in the range between the Curie temperatures where other methods are less reliable. Kobeko and Kurtzschatov⁴ measured the electrocaloric effect in Rochelle salt but they did not report numerical values. This study was undertaken to determine the validity of electrocaloric measurements and to obtain numerical

values for such parameters as χ_0 and ξ which appear in a phenomenological description of ferroelectricity in Rochelle salt.

EXPERIMENTS

Two crystals of Rochelle salt⁵ ($\text{NaKC}_4\text{H}_4\text{O}_6 \cdot 4\text{H}_2\text{O}$), each of which was about 2.5 cm on a side and 0.64 cm thick, were completely coated on their major faces with electrodes of silver paste, lightly cemented together, and suspended by cotton threads in a heavy copper chamber (Fig. 1). In order that the two crystals would not tend to stress one another when the electric field was applied, the crystals were oriented so that the piezoelectric strains in the top and bottom halves were in the same directions. To prevent evaporation of the water of crystallization, a portion of powdered Rochelle salt was deposited in the bottom of the chamber to raise the vapor pressure of water to the desired value. Dry gas was added at near atmospheric pressure to prevent arcing.

The electrocaloric temperature changes were measured by means of two copper-constantan thermocouples in series which were imbedded between the two crystals. The heat capacity of the thermocouples, cement, and electrodes was negligible compared to the heat capacity of the crystals. The copper chamber was employed as the reference junction J of these thermocouples.

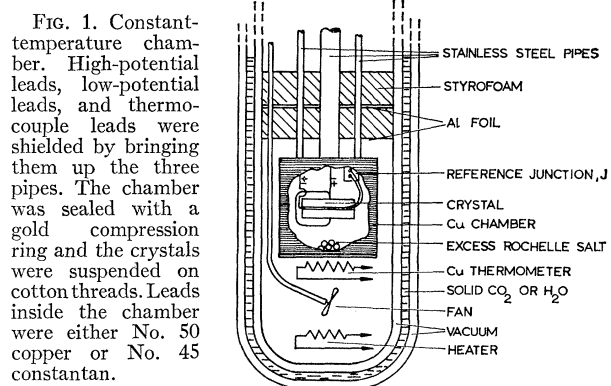


FIG. 1. Constant-temperature chamber. High-potential leads, low-potential leads, and thermocouple leads were shielded by bringing them up the three pipes. The chamber was sealed with a gold compression ring and the crystals were suspended on cotton threads. Leads inside the chamber were either No. 50 copper or No. 45 constantan.

¹ W. G. Cady, *Piezoelectricity* (McGraw-Hill Book Company, Inc., New York, 1946).

² H. Mueller, *Phys. Rev.* **57**, 829 (1940); **58**, 565 (1940).

³ A. F. Devonshire, *Suppl. Phil. Mag.* **3**, 85 (1954).

⁴ P. Kobeko and J. Kurtzschatov, *Z. Physik* **66**, 192 (1930).

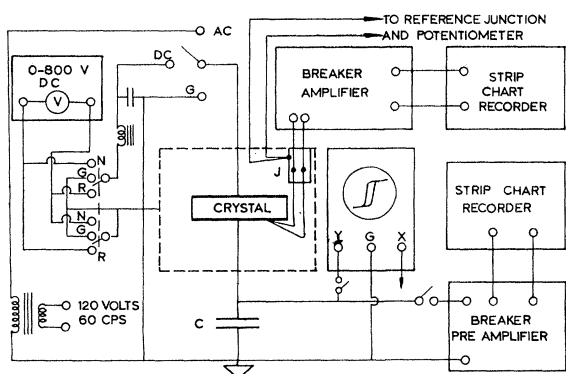


FIG. 2. Circuit for electrocaloric and dielectric hysteresis measurements. C was a polystyrene film capacitor, 0.5 to 7.5 μF . The X amplifier of the oscilloscope was connected through an attenuator and phase-adjusting network to the alternating voltage. The necessary shielding is not shown.

Multiple copper leads conducted the thermoelectric signal to a breaker amplifier and a strip-chart recorder. The circuit had a sensitivity of about 1.7×10^{-4} deg/div and a background noise, primarily Johnson noise⁶ in the input circuit, of ± 0.5 div. The electrocaloric temperature changes could be read to less than 10^{-4} deg. The response time was about one second.

The temperature of the copper chamber (and the reference junction J) was measured with another copper-constantan thermocouple and a potentiometer. The temperature of the chamber was regulated with a copper resistance thermometer and Mueller bridge, the unbalanced bridge signal activating a conventional galvanometer-phototube-heater arrangement.

Changes in electrical polarization were observed by means of a high-resistance amplifier connected across a polystyrene film capacitor C , as shown in Fig. 2. A circuit similar to that of Sawyer and Tower⁷ permitted observation of the hysteresis cycle at 60 cps for survey and comparison. This circuit was also used to determine the validity and speed of response of the thermocouple measurements: A 60-cps voltage was applied to the crystal for a known period and the energy supplied to the crystal as determined from a photograph of the hysteresis loop was compared with the energy supplied to the crystal as determined from the thermocouple readings.

The thermocouple-amplifier arrangement proved to be sufficiently sensitive to permit two typical types of measurements: (1) the "single-step" method in which the applied field was switched completely on or off, and (2) a "point-by-point" method in which the hysteresis cycle was traversed by a series of steps in the applied field, one step every two minutes. In each case the corresponding changes in temperature and charge were observed on the strip-chart recorders

(Fig. 2). Representative results of the single-step method are shown in Fig. 3, those of the point-by-point method in Fig. 4.

Because electrical measurements of the polarization include the combined contributions of volume polarization and residual conduction charges, values of P must be determined from measured changes in P and a reliable reference, the polarization at the extreme ends of the hysteresis loop. Moreover, it is necessary to correct for the unipolarity that exists in some crystals of Rochelle salt^{1,8}; the dashed horizontal axes for the hysteresis loops shown in Fig. 4 are uncorrected for unipolarity and stray residual charge.

The speed of response in recording the changes of both temperature and polarization was sufficiently fast to permit identification and elimination of occasional spurious effects such as switching pulses. The chart records were invaluable for recognizing slow changes in polarization and for extrapolating the temperature backward to correct for nonadiabatic conditions.

RESULTS AND DISCUSSION

Although Eq. (1a) is not suitable for determining the coefficients of the phenomenological description, it can be used to evaluate the validity of the electrocaloric measurements. Near T_m , the temperature of maximum spontaneous polarization P_s , $(\partial P/\partial T)_E$ is approximately equal to $(\partial P_s/\partial T)$, and the measured electrocaloric temperature change ΔT should be proportional to ΔE and should change from positive to negative as the crystal is cooled through T_m . Values of $\Delta P/\Delta T$ determined from electrocaloric measurements and Eq. (1a) are shown by the short dashed lines of Fig. 6(a). Agreement with values of $\partial P_s/\partial T$ is evident

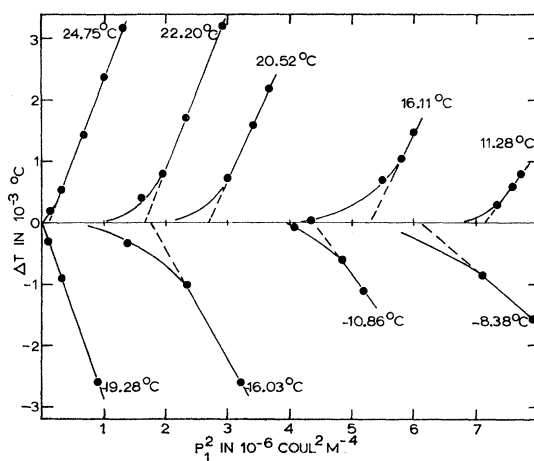


FIG. 3. Average electrocaloric temperature changes which accompanied single-step adiabatic depolarization from normal and reversed polarization. Values of polarization have been corrected for unipolarity and residual charge.

⁶ J. B. Johnson, Phys. Rev. 32, 97 (1928).

⁷ C. B. Sawyer and C. H. Tower, Phys. Rev. 35, 269 (1930).

⁸ K. N. Karmen, Kristallografiya 6, 426 (1961) [translation: Soviet Phys.—Cryst. 6, 336 (1962)].

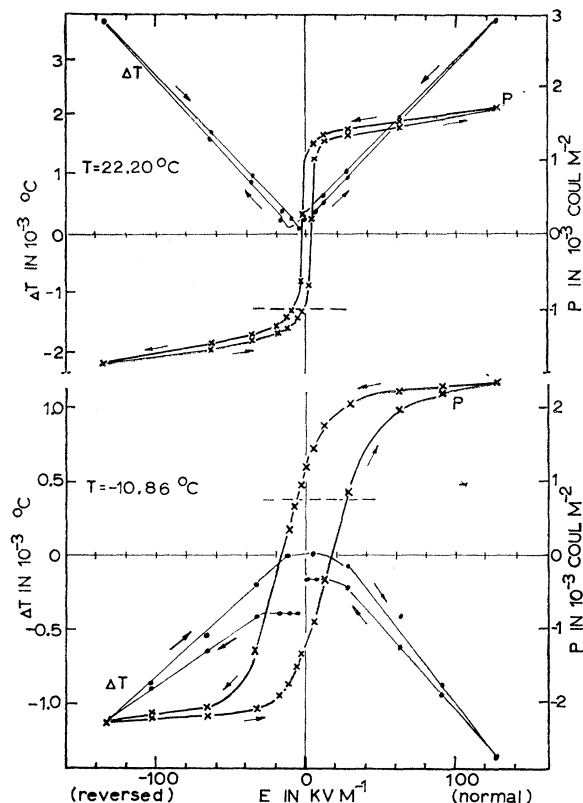


FIG. 4. Representative point-by-point measurements of the electrocaloric effect and dielectric hysteresis. Each point on the curves represents the cumulative ΔT or ΔP from an arbitrary initial value; several cycles were run before data were recorded. The error of closure of the ΔT curve at -10.86°C is due primarily to the pronounced irreversible effects at this temperature.

in this region. These lines are displaced vertically above P_s because the values of $\Delta P/\Delta T$ were measured in the reversible region near the ends of the hysteresis loops. The deviation between the measured slopes and $\partial P_s/\partial T$ near the Curie temperatures is to be expected because, for a substance whose transition to the ferroelectric state is of second order, the absolute value of $(\partial P/\partial T)_E$ decreases with E .³ These results are consistent with those of Kobeko and Kurtschatov⁴ and indicate freedom from serious errors associated with induced piezoelectric strains.

Equation (5), which is derived from Eq. (1b), contains the important parameter χ_0 . For finite changes in polarization, ΔT is much smaller than T and Eq. (5) becomes

$$\Delta T = (T/2C_P)(\partial\chi_0/\partial T)_P(P_2^2 - P_1^2), \quad (6)$$

where P_1 and P_2 are the initial and final values of the polarization, respectively. Thus, for a single-step depolarization, a plot of ΔT against P_1^2 should give a straight line whose slope is characteristic of the initial temperature and whose intercept on the polarization axis is P_s^2 as shown in Fig. 3. The deviations of the curves from straight lines at lower values of P (or E) is

attributed primarily to the misalignment of the polarized regions at lower field strengths and irreversible effects.

The values of P_s which were determined by extrapolating the linear portions of the single-step electrocaloric measurements (Fig. 3) together with those which were determined from the hysteresis loops are shown in Fig. 6(a). As the Curie temperatures are approached, the electrocaloric temperature changes become large and irreversible effects become small. As a result, the straight-line portions of the curves of Fig. 3 are dominant for electrocaloric measurements close to the Curie temperatures and the intercepts on the polarization axis can be determined rather accurately; therefore, the electrocaloric measurements yield accurate values for P_s near the Curie temperatures, just where determinations of P_s from the hysteresis loops are inaccurate.⁹ It follows that the ferroelectric Curie temperatures (the temperatures at which P_s disappears) can be most accurately determined by electrocaloric measurements. An analogous situation exists for ferromagnetism.

Far away from the Curie temperatures it is difficult to decide whether the curves of Fig. 3 have attained their maximum slope for the maximum field strengths used. Therefore, the point-by-point measurements of ΔT were plotted in a manner which would assist in making this decision; $\Delta T/\Delta(P^2)$, which is equivalent to the slope of the curves of Fig. 3, was plotted against P^2 , with the result shown in Fig. 5. The results of both methods are plotted in Fig. 6(b) and are reasonably well represented by the linear relationship,

$$\Delta T = b(T - T_m)\Delta(P^2), \quad (7)$$

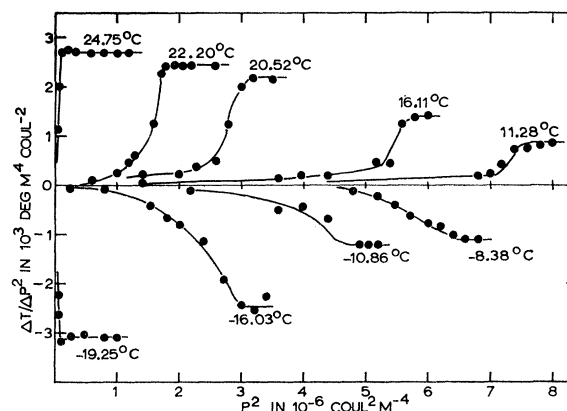


FIG. 5. Average electrocaloric temperature changes which accompanied point-by-point adiabatic polarization and depolarization in both the normal and reversed regions. The values were plotted to exhibit the saturation values of $\Delta T/\Delta(P^2)$. Large anomalies due to irreversible wall motions and/or misaligned regions are evident at low fields.

⁹ R. Becker and W. Döring, *Ferromagnetismus* (Julius Springer-Verlag, Berlin, 1939)

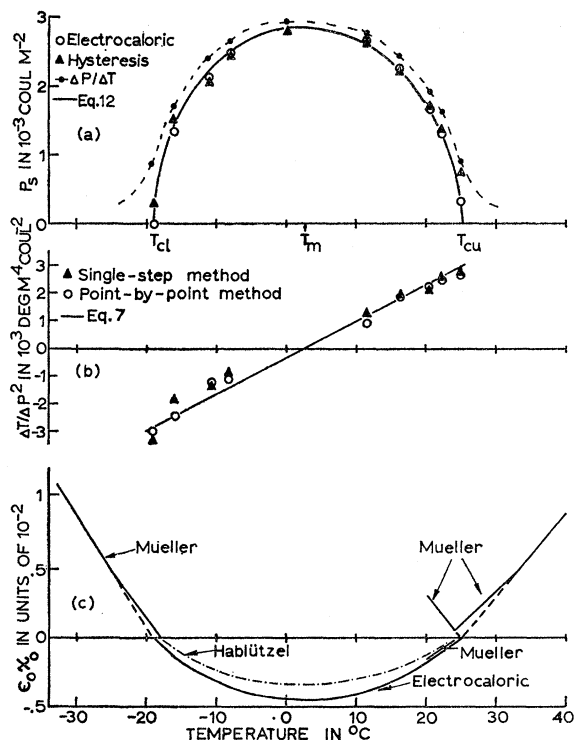


FIG. 6. (a) Comparison of Eq. (12) with values of P_s determined from hysteresis loops and from extrapolation of the linear portions of the electrocaloric measurements shown in Fig. 3. Values of $\Delta P/\Delta T$ were obtained from the electrocaloric effect, Eq. (1a). (b) Comparison of Eq. (7) with values determined from the single-step measurements and from saturation values of $\Delta T/\Delta(P^2)$ obtained by the point-by-point measurements. (c) Comparison of Mueller's susceptibility data [his $1/(4\pi\chi)$ in the paraelectric regions and $-1/(8\pi\chi)$ in the ferroelectric region] and Hablützel's susceptibility data [$-1/(2K)$ in the ferroelectric region] with the values obtained from the electrocaloric effect.

in which b is a constant and T_m is the temperature of maximum P_s .

Comparison of the experimental curve, Eq. (7), with Eq. (6) yields

$$(\partial\chi_0/\partial T)_P = 2bC_P(T - T_m)/T. \quad (8)$$

This expression, plus the knowledge that χ_0 must be zero at the Curie temperatures, gives

$$\chi_0 = 2bC_P[(T - T_c) - T_m \ln(T/T_c)]. \quad (9)$$

This expression must give the same value of χ_0 whether the upper or lower Curie temperature (T_{cu} or T_{cl}) is used; hence,

$$T_m = (T_{cu} - T_{cl})/\ln(T_{cu}/T_{cl}) \quad (10)$$

Thus, both b and T_m of Eq. (9) can be found from electrocaloric measurements. Their values are $b = 128 \text{ m}^4/\text{C}^2$ and $T_m = 2.5^\circ\text{C}$. The specific heat, $C_P = 2.30 \times 10^6 \text{ J/m}^3\text{deg}$, was determined from Wilson's measurements.¹⁰ Figure 6(c) displays the values of χ_0 as de-

termined from Eq. (9) throughout the ferroelectric range along with the values of χ_0 determined from the low-field differential susceptibility measurements of Mueller¹¹ and Hablützel.¹² The relationship between χ_0 and χ_p , the low-field susceptibility in the paraelectric range, is from Eq. (4)

$$1/\chi_p = \epsilon_0(\partial E/\partial T)_T = \epsilon_0\chi_0, \quad (11)$$

where the higher order terms have been neglected.

Setting $E=0$ in Eq. (4) and neglecting higher order terms of the polarization gives a relationship,³ $P_s = -\chi_0/\xi$, which in this case becomes

$$P_s^2 = (2bC_P/\xi)[(T_c - T) + T_m \ln(T/T_c)]. \quad (12)$$

Since $P_s(T)$ is known, ξ can now be determined. The solid curve of Fig. 6(a) is a plot of Eq. (12) with ξ chosen to fit the maximum experimental value of P_s . The value of ξ so determined is $0.64 \times 10^{14} \text{ Jm}^5/\text{C}^4$.

Following Devonshire³ and substituting $P_s^2 = -\chi_0/\xi$ into Eq. (4) gives an expression for χ_f , the low-field differential susceptibility in the ferroelectric range,

$$1/\chi_f = \epsilon_0(\partial E/\partial P)_T = -2\epsilon_0\chi_0. \quad (13)$$

Equations (11) and (13) give values of susceptibilities for isothermal processes, whereas the measurements give values for adiabatic processes. However, it can be shown by standard methods of thermodynamics¹³ that the ratio of the adiabatic susceptibility of a substance, χ_s , to its isothermal susceptibility, χ_T , is given by the ratio of its specific heats at constant polarization and constant field, $\chi_s/\chi_T = C_P/C_E$; for Rochelle salt C_P and C_E are equal to within a few tenths of 1%.¹⁰

The excess specific heat, $\Delta C = C_E - C_P$, would ordinarily be expected to furnish another means for determining the behavior of $\chi_0(T)$ but the value of ΔC for Rochelle salt is so small that its existence has been open to question on experimental grounds.^{10,14,15} Hoshino¹⁶ has pointed out a contradiction in the sign of ΔC predicted by Mueller's theory and by the Ehrenfest relation. The thermodynamic relation for the excess specific heat is

$$\Delta C = C_E - C_P = -T(\partial E/\partial T)_P(\partial P/\partial T)_E, \quad (14)$$

which with Eq. (4) gives for a short-circuited single crystal

$$\begin{aligned} \Delta C &= -TP(\partial\chi_0/\partial T)_P(\partial P/\partial T)_E \\ &= -T(\partial\chi_0/\partial T)_P dP_s^2/dT. \end{aligned} \quad (15)$$

Thus, to be consistent with the electrocaloric measurements, the excess specific heat ΔC should exhibit

¹¹ H. Mueller, Ann. N. Y. Acad. Sci. **40**, 321 (1940).

¹² J. Hablützel, Helv. Phys. Acta **12**, 489 (1939).

¹³ A. B. Pippard, *Classical Thermodynamics* (Cambridge University Press, New York, 1960).

¹⁴ A. A. Rusterholz, Helv. Phys. Acta **7**, 643 (1934); **8**, 39 (1935).

¹⁵ W. Bantle, Helv. Phys. Acta **15**, 373 (1942).

¹⁶ S. Hoshino, T. Mitsui, F. Jona, and R. Pepinsky, Phys. Rev. **107**, 1255 (1957).

¹⁰ A. J. C. Wilson, Phys. Rev. **54**, 1103 (1938).

positive maxima near both Curie temperature of about $4.9 \times 10^3 \text{ J/m}^3 \text{ deg}$ ($2.7 \times 10^{-3} \text{ J/g deg}$). This value is only 0.3% of C_P and would be difficult to observe. Positive values for ΔC at both Curie temperatures suggest that cooling through either transition produces a more ordered state, a conclusion that is consistent with some of the proposed models of ferroelectric Rochelle salt.^{17,18}

The agreement between the electrocaloric data and the susceptibility data is regarded as good, in particular, the values for the Curie temperatures, -19.2 and

25.2°C . This ferroelectric range is somewhat larger than the range ordinarily cited, but it agrees well with the extrapolated reciprocal susceptibility values of Mueller.²

There are discontinuities in the values of the slope dX_0/dT at both Curie temperatures which are possibly caused by ignoring the correction terms of higher order. These discontinuities are similar to those observed by Mueller² for dielectric, elastic, and piezoelectric properties. The slope, dX_0/dT , determined from the electrocaloric measurements near the upper Curie temperature is in excellent agreement with the values of $-1/(2\chi_f)$ determined from Mueller's susceptibility measurements¹¹ and in reasonable agreement with Hablützel's susceptibility measurements.¹²

¹⁷ E. T. Jaynes, *Ferroelectricity* (Princeton University Press, Princeton, New Jersey, 1952).

¹⁸ P. W. Forsbergh, Jr., *Encyclopedia of Physics*, edited by S. Flügge (Springer-Verlag, Berlin, 1956), Vol. XVII.

Properties of Ising Models Containing Dilute Impurities

F. H. STILLINGER, JR.

Bell Telephone Laboratories, Murray Hill, New Jersey

(Received 19 February 1963)

The coupling-parameter equations for spin-pair correlation functions are examined for field-free Ising models with coordination number four (including both two- and three-dimensional cases). By means of sets of identities discovered by Fisher, it proves possible to eliminate exactly all higher order correlation functions from the equations, in the event that only nearest-neighbor sites interact. As a result, one can rigorously show for this class of Ising models that each spin-pair correlation function (one spin partially coupled) is a linear combination of two independent functions of the coupling parameter, and that spatial dependence occurs only through their multiplicative factors. Only one relation between these spatial factors is available for each site-pair separation distance, so that the Ising problem in its usual interpretation (coupling-parameter unity) is not yet rigorously soluble by this approach. However, by using the correlation function for the fully coupled case itself as a second set of constraints, exact results can be obtained explicitly for the pair correlation function, and hence the solution thermodynamics, for dilute impurities coupled with arbitrary strength to their nearest neighbors.

I. INTRODUCTION

IN a previous paper,¹ the functional equations for the spin-pair correlation functions $\langle \mu_1 \mu_2 \rangle$ in field-free Ising models with arbitrary scalar interactions were derived by means of the single-site variable coupling scheme. The resulting formalism is the order-disorder analog of Kirkwood's^{2,3} coupling-parameter theory for liquid state molecular distribution functions. It has become traditionally expected in liquid theory, as developed by the coupling-parameter method, that the determining equation for the pair correlation function involves unknown higher order correlation functions. Also, it has tacitly been assumed that, if a closed exact expression for these higher order functions were available in terms of the desired pair function, the corresponding substitution would yield an equation that

should uniquely and exactly determine the important pair correlation function. The example provided below seems, however, to contradict this hope.

The "higher order functions" which arise in the coupling parameter (λ) analysis of order-disorder theory, are spin quadruplet correlations $\langle \mu_1 \mu_2 \mu_3 \mu_4 \rangle$. If only nearest neighbors in the lattice interact, then the quadruplet configurations are considerably restricted: Two sites must be nearest neighbors of a third.

The following section shows that the remaining quadruplet functions may exactly be replaced by pair correlation functions when the lattice has coordination number 4. This further restriction nevertheless still allows both two-dimensional (square) and three-dimensional (diamond, ice) lattices to be considered. The key element in this reduction is the relevant set of Fisher identities⁴ for these lattices, which are exhibited in detail below [Eqs. (8)–(14)].

¹ F. H. Stillinger, Jr., *Phys. Rev.* **126**, 1239 (1962).

² J. G. Kirkwood, *J. Chem. Phys.* **3**, 300 (1935).

³ T. L. Hill, *Statistical Mechanics* (McGraw-Hill Book Company, Inc., New York, 1956), Chap. 6.

⁴ M. E. Fisher, *Phys. Rev.* **113**, 969 (1959).